

Global Localization and Position Tracking of Automatic Guided Vehicles using passive RFID Technology

Christof Röhrig, University of Applied Sciences and Arts in Dortmund, christof.roehrig@fh-dortmund.de, Germany

André Heller, University of Applied Sciences and Arts in Dortmund, andre.heller@fh-dortmund.de, Germany

Daniel Heß, University of Applied Sciences and Arts in Dortmund, daniel.hess@fh-dortmund.de, Germany

Frank Künemund, University of Applied Sciences and Arts in Dortmund, frank.kuenemund@fh-dortmund.de, Germany

Abstract

Automated Guided Vehicles (AGVs) are used in warehouses, distribution centers and manufacturing plants in order to automate the internal material flow. Usually AGVs are designed to transport large and heavy transport units such as Euro-pallets or mesh pallets. Just-in-time inventory management and lean production requires small transportation units to enable one-piece-flow. A solution to meet these demands are small automatic vehicles for material transport, which can replace conventional conveyor systems or large AGVs. This paper presents an inexpensive solution for localization and tracking of small AGVs. Global localization is realized by detection of RFID transponders, which are integrated in the floor. The measurements of the RFID reader are fused with data from wheel encoders using Quantized Kalman filtering. The paper presents results from experiments with a NaviFloor® installation. The experiments show, that the proposed Quantized Kalman Filter provides a similar localization accuracy compared to a Monte Carlo Particle Filter, but with much lower computational expense.

1 Introduction

Just-in-time inventory management and short production cycles require flexible material flow as well as usage of small transportation units [1]. These demands can be met by using small Automated Guided Vehicles (AGVs). Several companies have introduced small AGVs for logistic applications. Examples are “The Kiva Mobile Fulfillment System (MFS)”, “ADAM™ (Autonomous Delivery and Manipulation)”, Grenzebach G-Com and G-Pro, and Adept Lynx. Furthermore, in several research projects small low cost AGVs are developed. Examples are “KARIS Kleinskaliges Autonomes Redundantes Intralogistik System”, KaTe “Kleine autonome Transporteinheiten” and LOCATIVE “Low Cost Automated Guided Vehicle” [2].

Inexpensive localization of small AGVs is an important issue for many logistic applications and object of current research activities. A solution for low cost localization is the dual use of technologies, which are needed for the operation of the vehicles. One example is the usage of IEEE 802.15.4a for communication as well as for global localization and laser range finders for safety as well as for detecting landmarks and local localization [3].

In several low cost low weight AGVs safety laser range finders are not implemented, because of their relatively high cost. A possible solution for global localization is the usage of auto-ID technology as artificial landmarks. The Kiva MFS and the Grenzebach G-Com use 2D bar codes on the floor, which can be detected with a camera by the AGVs [4]. These bar codes specify the pathways and guarantee accurate localization. Drawbacks of this solution are the risk of polluting the bar codes and the need for predefined pathways, which restrict the movements of the

AGVs. Another possible solution for global localization is the usage of Radio Frequency Identification (RFID) technology as artificial landmarks. Passive RFID technology is often used in logistics and warehouse management for object identification and tracking. Typically, the field of application is defined by the detection range of the RFID transponders, which depends on the operation frequency. Low frequency (LF) and high frequency (HF) tags operate in the near field region with inductive coupling and therefore support a much lower detection range than ultra high frequency (UHF) tags, which operates in the far field using backscattering. Usually LF or HF technology is used for self-localization and UHF technology is used for object identification in logistics applications [5] and service robotics [6].

The basic idea of using passive RFID transponders as artificial landmarks for self-localization of mobile systems is not new. LF RFID transponders are used to mark a predefined pathway for navigation of AGVs in industry since more than two decades [7]. For this purpose, the transponders are embedded in the ground along the pathway of the vehicles. LF transponders can be detected by RFID readers, which are attached at the vehicles. Detected transponder are compared with a map that contains serial numbers of RFID transponders along with their corresponding positions. The control system of the AGV interpolates a trajectory to the next transponder on the pathway and controls steering and speed. Odometry is used to move from one transponder to the next one. Thus, the maximum transponder distance depends on accuracy of odometry and on expected disturbances.

A known disadvantage of using LF RFID transponders for AGV navigation is the limited possible speed of the vehicle caused by the low data transfer rate of LF transponders.

Also LF transponders are comparatively expensive and the ground must be prepared with holes for these transponders [8]. Owing to the cost of installation and material, the transponders are installed on the pathway of the vehicles only.

An inexpensive option is the usage of cheap standard HF RFID transponders in the floor. The cost of a passive transponder is less than 0.2 €. A commercially available product, which employs passive HF RFID transponders in a floor, is the NaviFloor[®] manufactured by Future-Shape [9].

The main contribution of this paper is the development of a localization algorithm, which fuses the information from RFID readings with odometry using Quantized Kalman filtering. Only an inexpensive and small HF RFID reader and wheel encoders are needed for the proposed localization algorithm. The localization accuracy of the proposed algorithm is comparable to the accuracy of a Monte Carlo Particle Filter, but requires less computations. Furthermore, this paper extends the motion model for omnidirectional vehicles we have presented in [3]. The motion model considers uncertainties caused by inaccuracies in mechanics and speed control of the wheels.

The rest of the paper is organized as follows: Sec. 2 presents related work. In Sec. 3, the characteristics of the NaviFloor[®] are described. In Sec. 5, a motion model for omnidirectional Mecanum based vehicles is developed. The localization algorithm based on Quantized Kalman filtering is developed in Sec. 6. Experimental results are presented in Sec. 7. Finally, the conclusions are given in Sec. 8.

2 Related Work

In order to allow free navigation of AGVs, some research on RFID localization using low cost standard passive RFID tags have been done. Bayesian filtering is a solution for estimation of position and heading (pose) of a mobile robot by fusing odometry with RFID readings. Due to the highly non-Gaussian probability distribution of RFID tag readings, usually Particle Filters (PF) are used for this purpose [10]. Main drawback of the PF is the computational expense associated with it. Thus, there is some effort to replace the PF with methods based on Kalman filtering. Lee et al. have developed a Gaussian measurement model for UHF RFID transponders embedded in the floor, which is suitable for Kalman filtering [11]. Its application in a Kalman Filter has less computational expense, but provides not the same localization accuracy as a PF.

RFID measurements provide quantized measurements, which can be considered also as noisy dynamic constraints [12]. Boccadoro et. al. propose a Constrained Kalman Filter for global localization of mobile robots using UHF RFID technology and odometry [13]. In that research, the tags are placed at the walls in an indoor environment. DiGiampaolo and Martinelli have developed a Quantized Extended Kalman Filter algorithm for localization on mobile robots using UHF RFID tags at the ceiling [14]. Lev-

ratti et. al. propose a localization algorithm for robotic lawnmowers based on a modified Constrained Kalman Filter, that merges odometry with UHF RFID transponders, which are placed at the border of the working area [15]. For self-localization of mobile systems, the usage of HF transponders in the floor has some advantages over the usage of long range UHF technology at the walls or the ceiling. Usually the detection area is smaller and therefore the localization accuracy is better compared to long range UHF technology. Owing to the lower operation range, HF technology can be used with smaller antennas and lower radio power. This allows the operation in sensitive environments like hospitals. Furthermore HF technology is better applicable in small low cost AGVs, owing to the smaller size and lower power consumption compared to UHF technology.

HF RFID technology behaves different from long range UHF RFID technology, that is investigated in the research mentioned above, and therefore needs different modeling. In particular, floor placed HF RFID transponders have a nearly binary detection characteristic, where the detection area depends mainly on size and shape of the reader's antenna.

There is some research on technical aspects of self-localization on HF RFID tagged floor like antenna design [8], [16], antenna placement on the vehicle, [17], [18], transponder placement on the floor [19], [20], [21], and optimal detection range of the reader [22].

Since HF RFID technology gives information about the position only, there is some research on detection the heading of a mobile robot, while the robot is moving. Park and Hashimoto have proposed an algorithm that estimates the heading of a mobile robot using the read time of a RFID system [23]. They measure the time a RFID tag is detected, while the robots moves over the tag. Another possible solution for estimation of the heading is the Hough transform proposed in [24]. In that research, the moving space is transformed into an image and the position of the detected tags are features in the image.

Bayesian filtering is a solution for estimating the heading of a mobile robot considering the history of movements. Kodaka et al. apply a PF for pose estimation of a mobile robot using floor based RFID transponder and odometry [25]. Choi et al. propose the fusion of ultrasonic sensors, odometry and readings of HF RFID transponders, which are integrated in the floor [26].

3 NaviFloor[®]

The NaviFloor[®] is a glass fiber reinforcement in which passive HF RFID transponders are embedded. The NaviFloor[®] underlay is delivered in rolls including a map of the embedded RFID tags, simplifying the installation. NaviFloor[®] is specially developed for installation beneath artificial resin or terrazzo flooring, tiles or elastic flooring. It is pressure-resistant up to 45 N/mm² and withstands even heavy AGVs or fork lift trucks.

We have installed a NaviFloor[®] in our robotics lab. **Figure 1** shows a picture during the installation proce-

ture. The RFID tags are installed in a grid of 25 cm. The whole installation includes nearly a thousand RFID tags.



Figure 1: NaviFloor® Installation in our robotics lab

The tags embedded in the NaviFloor® have a rectangular shape $45 \text{ mm} \times 45 \text{ mm}$. NXP chips I-CODE SLI are integrated in the transponders. The transponders are compliant to ISO 15693 and communicate in the 13.56 MHz HF band.

4 Problem Formulation

We consider the problem of localizing a vehicle in a known environment. The vehicle is equipped with a RFID reader and moves over a floor with n RFID transponders. The position of the transponders is known a priori. The vehicle moves in 2D space, the pose of the vehicle is defined as $\mathbf{x} = (x, y, \theta)^T$. If a transponder $T_i \in \{T_1, \dots, T_n\}$ is in range of the reader, it is detected by the vehicle. The area where a transponder T_i can be detected by the reader is the detection area \mathcal{A}_i . The probability of detecting a transponder T_i at a position $\mathbf{z} = (x, y)^T$ inside the detection area \mathcal{A}_i of the reader is 1 and outside the area it is zero:

$$p(T_i, |\mathbf{z}) \begin{cases} 1 & \text{if } \mathbf{z} \in \mathcal{A}_i \\ 0 & \text{else} \end{cases} \quad (1)$$

False positive readings do not arise, owing to the short range of HF RFID technology. Therefore, the RFID reader can be treated as a binary detector if $\mathbf{z} \in \mathcal{A}_i$ or not. All positions \mathbf{z} that fall in the detection area lead to the same measurement. If more than one transponder can be detected at the same time, the intersection of the detection areas of all detected transponders has to be treated as measurement. Generalized, T_i can be assumed as a set of transponders and \mathcal{A}_i as the intersection of the associated detection areas. The orientation of the read antenna and therefore the heading of the vehicle may have an influence on the detection area. Thus in general, a RFID measurement can be interpreted as a *quantized measurement* of a

position, which depends on the pose of the vehicle:

$$\mathbf{z} = \mathbf{h}(\mathbf{x}, \mathbf{v}) \quad (2)$$

where \mathbf{z} is the quantized measurement, \mathbf{x} is the pose of the vehicle and \mathbf{v} is the measurement noise, that models additional sources of uncertainty:

- Communication delay between RFID reader and transponder: This delay is caused by limited data rate of the air interface and the collision avoidance procedure for multi tag readings.
- Communication delay between control system and RFID reader: This delay is caused by the processing time of the reader and the limited data rate on the interface to the reader.
- Variations in tag placement: Due to production tolerances of the NaviFloor® and manual placement, the position of the RFID tags may differ from regular grid.

The uncertainty in tag placement can be treated as Gaussian noise. The communication delays causes additional noise that depends on the speed of the vehicle.

Aim of the pose estimation is to obtain the probability density $p(\mathbf{x}_k | T_i, \mathbf{x}_{k-1}, \mathbf{u}_k) = p(\mathbf{x}_k | \mathbf{z}_k \in \mathcal{A}_i, \mathbf{x}_{k-1}, \mathbf{u}_k)$, where \mathbf{u}_k is the control input of the vehicle. This can be achieved by applying a Bayesian filter:

$$p(\mathbf{x}_k | \mathbf{z}_k \in \mathcal{A}_i, \mathbf{x}_{k-1}, \mathbf{u}_k) = \frac{p(\mathbf{z}_k \in \mathcal{A}_i | \mathbf{x}_k) p(\mathbf{x}_k | \mathbf{x}_{k-1}, \mathbf{u}_k)}{p(\mathbf{z}_k \in \mathcal{A}_i)} \quad (3)$$

where $p(\mathbf{z}_k \in \mathcal{A}_i | \mathbf{x}_k)$ can be obtained from sensor model (1) and (2) and $p(\mathbf{x}_k | \mathbf{x}_{k-1}, \mathbf{u}_k)$ is modeled by a motion model of the vehicle. A motion model for omnidirectional vehicles is developed in the Sec. 5. The implementation of (3) in a Particle Filter and a Quantized Extended Kalman Filter in described in Sec. 6.

5 Motion Model for Vehicles with Mecanum Wheels

In this section, a motion model for omnidirectional vehicles with Mecanum wheels is derived, which is suitable for poses estimation using an Extended Kalman Filter (EKF). The motion model is based on experiments with our Mecanum driven omnidirectional vehicles and extends the work presented in [3]. An omnidirectional vehicle is able to move in any direction and rotate around its z-axis at the same time. The motion models found in literature are limited to mobile robots with two degrees of freedom. The motion model is based on odometry measurements obtained from wheel encoders. Odometry can be treated as controls, because most vehicle control systems control the movements of the vehicle in a closed position control loop based on odometry. In this case, the command values of the control loop correspond directly to odometry. The movements of the vehicle are corrupted by disturbances caused by mechanical inaccuracies such as uneven floor,

wheel slippage and inaccuracies in the speed control of the wheels that lead to coupling errors. These disturbances will be treated as process noise.

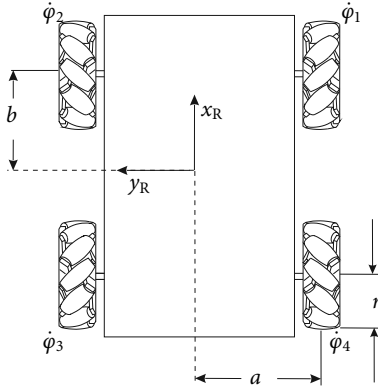


Figure 2: Omnidirectional vehicle with Mecanum wheels

The vehicle is equipped with Mecanum wheels and electronic drives, which provide three degrees of freedom. The omnidirectional vehicle possesses four motor driven Mecanum wheels. The wheel configuration of the mobile system is shown in **Figure 2**. The velocities in the vehicle (robot) frame $(\dot{x}_R, \dot{y}_R, \dot{\theta})$ are a function of the four wheel velocities $\dot{\varphi}_1 \dots \dot{\varphi}_4$:

$$\begin{pmatrix} \dot{x}_R \\ \dot{y}_R \\ \dot{\theta} \\ \dot{\varphi}_e \end{pmatrix} = \mathbf{J} \begin{pmatrix} \dot{\varphi}_1 \\ \dot{\varphi}_2 \\ \dot{\varphi}_3 \\ \dot{\varphi}_4 \end{pmatrix}, \quad \mathbf{J} = \frac{r}{4} \begin{pmatrix} 1 & 1 & 1 & 1 \\ -1 & 1 & -1 & 1 \\ \frac{1}{a+b} & \frac{-1}{a+b} & \frac{-1}{a+b} & \frac{1}{a+b} \\ \frac{4}{r} & \frac{4}{r} & \frac{-4}{r} & \frac{-4}{r} \end{pmatrix} \quad (4)$$

where r is the radius of the wheels, a and b are given by the dimension of the vehicle (see Figure 2). An angular error velocity $\dot{\varphi}_e \neq 0$ causes a coupling error of the wheels and thus additional wheel slippage. Eqn. (4) is used in the operating system of the vehicle to execute odometry. The inverse equation transforms velocities in vehicle frame into the wheel velocities:

$$\begin{pmatrix} \dot{\varphi}_1 \\ \dot{\varphi}_2 \\ \dot{\varphi}_3 \\ \dot{\varphi}_4 \end{pmatrix} = \mathbf{J}^{-1} \begin{pmatrix} \dot{x}_R \\ \dot{y}_R \\ \dot{\theta} \\ \dot{\varphi}_e \end{pmatrix} \quad (5)$$

Eqn. (5) is used in the operating system of the vehicle to control the speeds in vehicle frame. The control variable $\dot{\varphi}_e$ can be used to force the coupling error φ_e to zero [27]. For more details about the kinematics of the vehicle refer to [28].

Velocities in the vehicle frame can be transformed into the world frame, if the heading θ of the vehicle is known.

$$\dot{\mathbf{x}}_R = \mathbf{R}(\theta) \dot{\mathbf{x}}_W, \quad \Rightarrow \quad \dot{\mathbf{x}}_W = \mathbf{R}^{-1}(\theta) \dot{\mathbf{x}}_R \quad (6)$$

$$\text{with } \dot{\mathbf{x}}_W = \begin{pmatrix} \dot{x}_W \\ \dot{y}_W \\ \dot{\theta} \end{pmatrix}, \quad \dot{\mathbf{x}}_R = \begin{pmatrix} \dot{x}_R \\ \dot{y}_R \\ \dot{\theta} \end{pmatrix},$$

$$\mathbf{R}(\theta) = \begin{pmatrix} \cos \theta & \sin \theta & 0 \\ -\sin \theta & \cos \theta & 0 \\ 0 & 0 & 1 \end{pmatrix}$$

Between two time steps of odometry it is assumed, that the omnidirectional vehicle moves on a straight line while it rotates from θ_{k-1} to θ_k at the same time (see **Figure 3**). To simplify calculations, this movement is divided into three independent movements. First a rotation $\Delta\theta/2$, then a translation $(\Delta x, \Delta y)$ without rotation and finally again a rotation $\Delta\theta/2$.

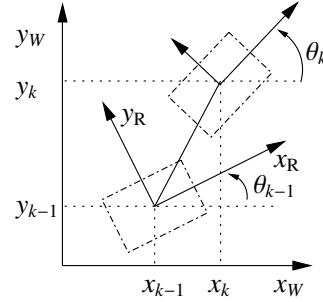


Figure 3: Movement of an omnidirectional vehicle

The movements described in directions of the vehicle frame can be calculated with (4) as:

$$\begin{pmatrix} \Delta x_R \\ \Delta y_R \\ \Delta \theta \\ \Delta \varphi_e \end{pmatrix} = \mathbf{J} \begin{pmatrix} \Delta \varphi_1 \\ \Delta \varphi_2 \\ \Delta \varphi_3 \\ \Delta \varphi_4 \end{pmatrix} \quad (7)$$

With these movements, the new pose in world frame $\mathbf{x}_k = (x_k, y_k, \theta_k)^T$ can be calculated based on the pose before the movement (\mathbf{x}_{k-1}) :

$$\begin{aligned} x_k &= x_{k-1} + \Delta x_R \cos(\theta_{k-1} + \frac{\Delta\theta}{2}) \\ &\quad - \Delta y_R \sin(\theta_{k-1} + \frac{\Delta\theta}{2}) \\ y_k &= y_{k-1} + \Delta x_R \sin(\theta_{k-1} + \frac{\Delta\theta}{2}) \\ &\quad + \Delta y_R \cos(\theta_{k-1} + \frac{\Delta\theta}{2}) \\ \theta_k &= \theta_{k-1} + \Delta\theta \end{aligned} \quad (8)$$

5.1 Uncertainty Modeling

The movements of the vehicle are corrupted by noise caused by mechanical inaccuracies. Experiments with the omnidirectional vehicle show that the noise is mainly caused by slippage of the Mecanum wheels. Since the slippage of the wheels depends on the rotational speed of the free spinning rollers, the uncertainty depends on the direction of the movement in vehicle frame. Therefore, it is assumed that the movements of the vehicle in vehicle frame are corrupted by independent noise ϵ_i :

$$\Delta \hat{x}_R = \Delta x_R + \epsilon_x, \quad \Delta \hat{y}_R = \Delta y_R + \epsilon_y, \quad \Delta \hat{\theta}_R = \Delta \theta_R + \epsilon_\theta \quad (9)$$

Furthermore, it is assumed that the noise ϵ_i is normally distributed with zero mean $\epsilon_i = \mathcal{N}(0, \sigma_i^2)$. The standard deviation σ_i is proportional to the displacement in the vehicle frame and changes in the coupling error $\Delta\varphi_e$:

$$\begin{pmatrix} \sigma_x \\ \sigma_y \\ \sigma_\theta \end{pmatrix} = \begin{pmatrix} \alpha_x^x & \alpha_x^y & \alpha_x^\theta & \alpha_x^e \\ \alpha_y^x & \alpha_y^y & \alpha_y^\theta & \alpha_y^e \\ \alpha_\theta^x & \alpha_\theta^y & \alpha_\theta^\theta & \alpha_\theta^e \end{pmatrix} \begin{pmatrix} \Delta x_R \\ \Delta y_R \\ \Delta \theta_R \\ \Delta \varphi_e \end{pmatrix} \quad (10)$$

The parameters α_i^j are vehicle-specific constants, which have to be identified by experiments.

With the additional noise, the motion model can be described as follows:

$$\mathbf{x}_k = \mathbf{f}(\mathbf{x}_{k-1}, \mathbf{u}_k, \mathbf{w}_k), \quad \text{with} \quad \mathbf{x}_k = \begin{pmatrix} x_k \\ y_k \\ \theta_k \end{pmatrix}, \quad (11)$$

$$\mathbf{u}_k = \begin{pmatrix} \Delta x_R \\ \Delta y_R \\ \Delta \theta_R \\ \Delta \varphi_e \end{pmatrix}, \quad \mathbf{w}_k = \begin{pmatrix} \epsilon_x \\ \epsilon_y \\ \epsilon_\theta \end{pmatrix}$$

$$\begin{aligned} x_k &= x_{k-1} + (\Delta x_R + \epsilon_x) \cos\left(\theta_{k-1} + \frac{\Delta\theta + \epsilon_\theta}{2}\right) \\ &\quad - (\Delta y_R + \epsilon_y) \sin\left(\theta_{k-1} + \frac{\Delta\theta + \epsilon_\theta}{2}\right) \\ y_k &= y_{k-1} + (\Delta x_R + \epsilon_x) \sin\left(\theta_{k-1} + \frac{\Delta\theta + \epsilon_\theta}{2}\right) \\ &\quad + (\Delta y_R + \epsilon_y) \cos\left(\theta_{k-1} + \frac{\Delta\theta + \epsilon_\theta}{2}\right) \\ \theta_k &= \theta_{k-1} + \Delta\theta + \epsilon_\theta \end{aligned} \quad (12)$$

5.2 Linearization

In order to use the motion model in an EKF, $\mathbf{f}(\bullet)$ has to be linearized. In the prediction step of the EKF, the estimated pose of the vehicle

$$\hat{\mathbf{x}}_k = \mathbf{f}(\hat{\mathbf{x}}_{k-1}, \mathbf{u}_k, \mathbf{0}) \quad (13)$$

and the covariance of the pose

$$\mathbf{P}_k = \mathbf{\Phi}_k \mathbf{P}_{k-1} \mathbf{\Phi}_k^T + \mathbf{W}_k \mathbf{Q}_k \mathbf{W}_k^T, \quad (14)$$

can be calculated based on $\mathbf{f}(\bullet)$ and its Jacobians $\mathbf{\Phi}_k$ and \mathbf{W}_k :

$$\mathbf{\Phi}_k = \frac{\partial \mathbf{f}}{\partial \mathbf{x}}(\hat{\mathbf{x}}_{k-1}, \mathbf{u}_k, \mathbf{0}) = \quad (15)$$

$$\begin{pmatrix} 1 & 0 & -\Delta x_R \sin \theta'_{k-1} - \Delta y_R \cos \theta'_{k-1} \\ 0 & 1 & \Delta x_R \cos \theta'_{k-1} - \Delta y_R \sin \theta'_{k-1} \\ 0 & 0 & 1 \end{pmatrix},$$

$$\text{with} \quad \theta' = \theta_{k-1} + \frac{\Delta\theta}{2}$$

$$\mathbf{W}_k = \frac{\partial \mathbf{f}}{\partial \mathbf{w}}(\hat{\mathbf{x}}_{k-1}, \mathbf{u}_k, \mathbf{0}) = \quad (16)$$

$$\begin{pmatrix} \cos \theta' & -\sin \theta' & -\frac{1}{2} \Delta x_R \sin \theta' - \frac{1}{2} \Delta y_R \cos \theta' \\ \sin \theta' & \cos \theta' & \frac{1}{2} \Delta x_R \cos \theta' - \frac{1}{2} \Delta y_R \sin \theta' \\ 0 & 0 & 1 \end{pmatrix}.$$

The process covariance matrix

$$\mathbf{Q}_k = \begin{pmatrix} \sigma_x^2 & 0 & 0 \\ 0 & \sigma_y^2 & 0 \\ 0 & 0 & \sigma_\theta^2 \end{pmatrix} \quad (17)$$

can be calculated using (10).

5.3 Motion Sampling Algorithm

Eqn. (12) can be used to develop the motion sampling algorithm, which is needed by the Monte Carlo localization procedure. Algorithm 1 shows the sequence of calculations to sample the particles.

1: **sample_motion_model**($\mathbf{x}_{k-1}, \mathbf{u}_k$)

$$2: \begin{pmatrix} \sigma_x \\ \sigma_y \\ \sigma_\theta \end{pmatrix} = \begin{pmatrix} \alpha_x^x & \alpha_x^y & \alpha_x^\theta & \alpha_x^e \\ \alpha_y^x & \alpha_y^y & \alpha_y^\theta & \alpha_y^e \\ \alpha_\theta^x & \alpha_\theta^y & \alpha_\theta^\theta & \alpha_\theta^e \end{pmatrix} \cdot \mathbf{u}_k$$

3: $\Delta \hat{x}_R = \Delta x_R + \mathbf{sample}(\sigma_x)$

4: $\Delta \hat{y}_R = \Delta y_R + \mathbf{sample}(\sigma_y)$

5: $\Delta \hat{\theta} = \Delta \theta + \mathbf{sample}(\sigma_\theta)$

6: $\hat{\theta}' = \theta_{k-1} + \Delta \hat{\theta} / 2$

7: $x_k = x_{k-1} + \Delta \hat{x}_R \cos \hat{\theta}' - \Delta \hat{y}_R \sin \hat{\theta}'$

8: $y_k = y_{k-1} + \Delta \hat{y}_R \cos \hat{\theta}' + \Delta \hat{x}_R \sin \hat{\theta}'$

9: $\theta_k = \theta_{k-1} + \Delta \hat{\theta}$

10: **return** $\mathbf{x}_k = (x_k, y_k, \theta_k)^T$

Algorithm 1: Motion sampling algorithm

6 Proposed Localization Algorithm

This section describes the pose estimation (see (3)) in two different types of Bayesian filters. As mentioned before, usually Particle filters are deployed in RFID localization algorithms, because of the highly nonlinear and quantized measurements by the RFID reader. A Particle Filter will be used as benchmark for our proposed localization algorithm based on Quantized Kalman filtering.

6.1 Measurement Update for Particle Filters

For global localization, the particle set is uniformly distributed over the operation area of the vehicle. Alternatively, after detecting the first tag, particles are uniformly distributed over the detection area of the detected tag. The motion update is executed according to Algorithm 1

The measurement update in a particle filter is straight forward (see also [25]). After the vehicle has detected a RFID transponder, the corresponding detection area is calculated. After that, each particle x_k^j is distributed through the measurement function (2) and then weighted with the associated probability ($w_j = p(T_i | z_k)$). In our case, the probability inside the detection area is $p(T_i | z_k \in \mathcal{A}_i) = 1$, outside the detection area zero ($w_j = 0$). If no particle falls inside the detection area ($\sum w_j \approx 0$), the particle set has to be reinitialized. In this case, the particles are uniformly distributed over the detection area \mathcal{A}_i . Otherwise, the particle set is normalized and resampled.

6.2 Measurement Update for Kalman Filters

In contrast to the Particle Filter, a Kalman Filter has to be initialized with a rough initial state of the vehicle. Since a RFID reading provides no information about the heading of the vehicle, at least two RFID readings are necessary to initialize the Kalman Filter. This initial procedure is a kind of map-matching between the initial local map of the vehicle processed by odometry and the global map including the tag positions. The heading can be estimated after detecting two RFID tags (T_i, T_j):

$$\hat{\theta}_k = \theta_k^1 + \text{atan2}(\Delta y, \Delta x) - \text{atan2}(\Delta y^1, \Delta x^1), \quad (18)$$

where θ_k^1 is the local heading while detecting the second tag, $\Delta x = x_j - x_i$, $\Delta y = y_j - y_i$ are the distances between the detected tags and $\Delta y^1, \Delta x^1$ are the distances of the trajectory traveled in the local map. θ_k^1 has to be considered, because an omnidirectional vehicle can move in any direction without changing its heading. The estimation of $\hat{\theta}_k$ is very rough, because $\Delta x, \Delta y$ are quantized with the grid size of the RFID tags.

After global localization, we apply Quantized Kalman filtering for position tracking. The detection of a transponder can be considered as a quantized measurement of a position ($z = \mathbf{h}(\mathbf{x}, \mathbf{v})$, $z \in \mathcal{A}_i$, see (2)). The size of the detection area \mathcal{A}_i is a measure of the uncertainty in the measurement. The probability is distributed uniformly:

$$p(\mathbf{z} | \mathbf{z} \in \mathcal{A}_i) = \begin{cases} \frac{1}{|\mathcal{A}_i|} & \text{if } \mathbf{z} \in \mathcal{A}_i \\ 0 & \text{else} \end{cases} \quad (19)$$

where $|\mathcal{A}_i|$ is the size of \mathcal{A}_i :

$$|\mathcal{A}_i| = \int_{\mathcal{A}_i} d\mathbf{z} \quad (20)$$

We apply the *Gaussian-Fit Algorithm* proposed by Curry [29, p. 23–25] to Extended Kalman filtering. The first and second moment of $p(\mathbf{z} | \mathbf{z} \in \mathcal{A}_i)$ are needed in the measurement update of the Quantized EKF (QEKF). For notational convenience let

$$\boldsymbol{\mu}_i = \mathbb{E}(\mathbf{z} | \mathbf{z} \in \mathcal{A}_i), \quad \boldsymbol{\Sigma}_i = \text{cov}(\mathbf{z} | \mathbf{z} \in \mathcal{A}_i).$$

The mean

$$\boldsymbol{\mu}_i = \int p(\mathbf{z} | \mathbf{z} \in \mathcal{A}_i) \mathbf{z} d\mathbf{z} = \frac{1}{|\mathcal{A}_i|} \int_{\mathcal{A}_i} \mathbf{z} d\mathbf{z} \quad (21)$$

and the covariance

$$\begin{aligned} \boldsymbol{\Sigma}_i &= \int \Delta \mathbf{z} \Delta \mathbf{z}^T p(\mathbf{z} | \mathbf{z} \in \mathcal{A}_i) d\mathbf{z} \quad (22) \\ &= \frac{1}{|\mathcal{A}_i|} \int_{\mathcal{A}_i} \Delta \mathbf{z} \Delta \mathbf{z}^T d\mathbf{z} \quad \text{with } \Delta \mathbf{z} = \mathbf{z} - \boldsymbol{\mu}_i \end{aligned}$$

of all detection areas \mathcal{A}_i can be calculated in advance using numerical integration. Additional measurement noise caused by communication delays and tag misplacement

due to production tolerances can be modeled with a random variable \mathbf{v}_k . We assume that \mathbf{v}_k is normally distributed with zero mean ($\mathbf{v}_k \sim \mathcal{N}(\mathbf{0}, \mathbf{R}_k)$).

Before the measurement update is performed, we check the innovation of the measurement T_i . If $\hat{\mathbf{z}} = \mathbf{h}(\hat{\mathbf{x}}_k, \mathbf{0}) \in \mathcal{A}_i$, the innovation is zero and the detection of T_i gives no additional information. Thus no measurement update is performed. The measurement update is performed only, if $\hat{\mathbf{z}} \notin \mathcal{A}_i$. The measurement update is similar to the standard EKF algorithm:

$$\mathbf{K}_k = \mathbf{P}_k \mathbf{H}_k^T (\mathbf{H}_k \mathbf{P}_k \mathbf{H}_k^T + \mathbf{R}_k)^{-1} \quad (23)$$

$$\hat{\mathbf{x}}_k^+ = \hat{\mathbf{x}}_k + \mathbf{K}_k (\boldsymbol{\mu}_i - \mathbf{h}(\hat{\mathbf{x}}_k, \mathbf{0})) \quad (24)$$

$$\mathbf{P}_k^+ = (\mathbf{I} - \mathbf{K}_k \mathbf{H}_k) \mathbf{P}_k + \mathbf{K}_k \boldsymbol{\Sigma}_i \mathbf{K}_k^T \quad (25)$$

where \mathbf{K}_k is the Kalman gain and $\mathbf{H}_k = \frac{\partial \mathbf{h}}{\partial \mathbf{x}}(\hat{\mathbf{x}}_k, \mathbf{0})$. The derivation of (25) can be found in [29, p. 12]

7 Experimental Evaluation

7.1 Experimental Setup

We use a SkyeModule M1 as RFID reader. The HF antenna of the reader has a rectangular shape 38 mm \times 40 mm. A transponder is detected, if the antennas of transponder and reader have a small overlap. With maximum overlap, the detection range between reader and antenna is 50 mm. We have mounted the reader at a distance of 30 mm to the floor in the origin of the vehicle frame. At this distance, the detection area of the reader has a circular shape with a diameter of 90 mm (see **Figure 4**). The orientation of the reader has only a small impact on the detection area.

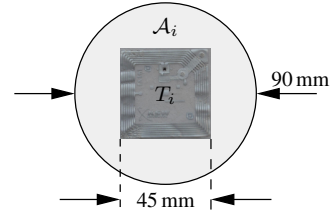


Figure 4: Detection area \mathcal{A}_i of RFID transponder T_i

The RFID transponders in the floor are placed in a regular grid of 250 mm. Thus, at most one RFID transponder can be detected at any moment. In case of a circular shape, $\boldsymbol{\mu}_i$ is the center of the circle and

$$\boldsymbol{\Sigma}_i = \begin{pmatrix} \frac{R^2}{4} & 0 \\ 0 & \frac{R^2}{4} \end{pmatrix}$$

where R is the radius of the circle. The measurement function

$$\mathbf{z}_k = \mathbf{h}(\mathbf{x}_k, \mathbf{v}_k) = \mathbf{H} \mathbf{x}_k + \mathbf{v}_k \quad \text{with } \mathbf{H} = \begin{pmatrix} 1 & 0 & 0 \\ 0 & 1 & 0 \end{pmatrix}$$

is linear with additional measurement noise $\mathbf{v}_k \sim \mathcal{N}(\mathbf{0}, \mathbf{R}_k)$.

7.2 Experimental Results

We have made some experiments with one of our omnidirectional vehicles in our lab on the NaviFloor® installation. **Figure 5** shows results from one of our experiments. The vehicle moves a square path $2\text{ m} \times 2\text{ m}$ several times with a velocity of 350 mm/s . The heading is constant during the whole movement ($\theta = 270^\circ$). The path of the vehicle is controlled by odometry and gyroscope. The sample time of odometry is 3 ms and the sample time of the RFID reader is 20 ms . Global localization of the vehicle is realized with the proposed QEKF that fuses data from wheel encoders and RFID readings. Pose estimation is started after the second RFID tag is detected. The initial state of the QEKF is estimated as described in Sec. 6.2. The estimated position of the vehicle is printed in red. The pose of the robot estimated by odometry only is shown in green. In Figure 5 RFID tags that are detected by the vehicle are shown as black circles.

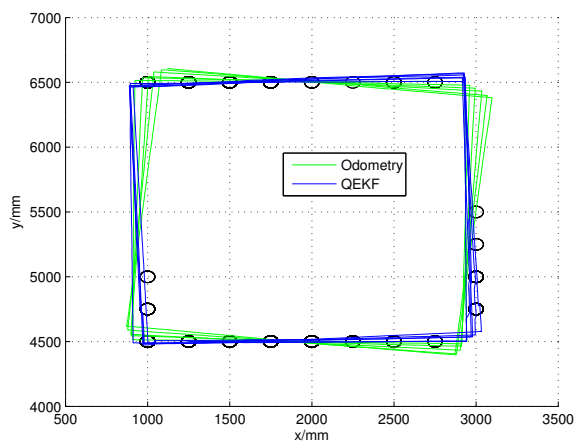


Figure 5: Experimental results

The accuracy of the QEKF is similar to a PF but with much less computational expense. Since no exact ground truth is provided by our experimental equipment, exact measures can not be given. It is estimated, that the mean error of the pose estimate in our experiments is lower than 30 mm .

8 Conclusions

In this paper, we have presented a localization algorithm based on Quantized Kalman filtering that fuses sensory data from wheel encoders with RFID readings. The RFID readings are assumed as quantized measurements of the vehicle's position. This assumption considers the quantized nature of floor-installed HF RFID readings. The detection area is approximated by a normal distribution using the Gaussian-Fit Algorithm. The localization accuracy of the QEKF is similar to a PF but with much less computational expense. The localization concept is suitable for small and inexpensive AGVs, since the vehicles need only a inexpensive and small HF RFID reader.

References

- [1] K. Furmans, M. Schleyer, and F. Schönung. A Case for Material Handling Systems, Specialized on Handling Small Quantities. In *Proceedings of the 10. International Material Handling Research Colloquium (IMHRC 2008)*, Dortmund, Germany, May 2008.
- [2] Thomas Kirks, Jonas Stenzel, Andreas Kamagaew, and Michael ten Hompel. Cellular transport vehicles for flexible and changeable facility logistics systems. *Logistics Journal*, 2192(9084):1, 2012.
- [3] C. Röhrig, D. Heß, C. Kirsch, and F. Künemund. Localization of an Omnidirectional Transport Robot Using IEEE 802.15.4a Ranging and Laser Range Finder. In *Proceedings of the 2010 IEEE/RSJ International Conference on Intelligent Robots and Systems (IROS 2010)*, pages 3798–3803, Taipei, Taiwan, October 2010.
- [4] E. Guizzo. Three Engineers, Hundreds of Robots, one Warehouse. *IEEE Spectrum*, 7:27–34, 2008.
- [5] Guidong Liu, Wensheng Yu, and Yu Liu. Resource management with RFID technology in automatic warehouse system. In *Intelligent Robots and Systems, 2006 IEEE/RSJ International Conference on*, pages 3706–3711, 2006.
- [6] Thomas Kämpke, Boris Kluge, and Matthias Strobel. Exploiting RFID capabilities onboard a service robot platform. In Erwin Prassler, Marius Zöllner, Rainer Bischoff, Wolfram Burgard, Robert Haschke, Martin Hägele, Gisbert Lawitzky, Bernhard Nebel, Paul Plöger, and Ulrich Reiser, editors, *Towards Service Robots for Everyday Environments*, volume 76 of *Springer Tracts in Advanced Robotics*, pages 215–225. Springer Berlin Heidelberg, 2012.
- [7] Götting KG. Introduction transponder positioning. <http://www.goetting-agv.com/components/transponder/introduction>.
- [8] M. Baum, B. Niemann, and L. Overmeyer. Passive 13.56 MHz RFID transponders for vehicle navigation and lane guidance. In *Proceedings of the 1st International EUR AS IP Workshop on RFID Technology*, pages 83–86, 2007.
- [9] A. Steinhage and C. Lauterbach. SensFloor® and NaviFloor®: Large-area sensor systems beneath your feet. In N. Chong and F. Mastrogianni, editors, *Handbook of Research on Ambient Intelligence and Smart Environments: Trends and Perspectives*, pages 41–55. Hershey, PA: Information Science Reference, 2011.
- [10] P. Vorst and A. Zell. Particle filter-based trajectory estimation with passive UHF RFID fingerprints in unknown environments. In *IEEE/RSJ International Conference on Intelligent Robots and Systems, 2009. IROS 2009.*, pages 395–401. IEEE, 2009.

- [11] Jewon Lee, Youngsu Park, Daehyun Kim, Minhoo Choi, Taedong Goh, and Sang-Woo Kim. An efficient localization method using RFID tag floor localization and dead reckoning. In *Control, Automation and Systems (ICCAS), 2012 12th International Conference on*, pages 1452–1456, 2012.
- [12] Costanzo Manes and Francesco Martinelli. State estimation under quantized measurements: a sigma-point bayesian approach. In *IEEE Conf. on Decision and Control (CDC 2013)*, pages 5024–5029, Florence, Italy, December 2013.
- [13] Mauro Boccadoro, Francesco Martinelli, and Stefano Pagnottelli. Constrained and quantized kalman filtering for an RFID robot localization problem. *Autonomous Robots*, 29(3-4):235–251, 2010.
- [14] Emidio DiGiampaolo and Francesco Martinelli. A passive UHF-RFID system for the localization of an indoor autonomous vehicle. *Industrial Electronics, IEEE Transactions on*, 59(10):3961–3970, 2012.
- [15] Alessio Levratti, Matteo Bonaiuti, Cristian Secchi, and Cesare Fantuzzi. An inertial/RFID based localization method for autonomous lawnmowers. In *Proceedings of the 10th IFAC Symposium on Robot Control, IFAC SYROCO 2012*, pages 145–150, Dubrovnik, Croatia, September 2012.
- [16] M.Y. Ahmad and A.S. Mohan. Novel bridge-loop reader for positioning with HF RFID under sparse tag grid. *Industrial Electronics, IEEE Transactions on*, 61(1):555–566, 2014.
- [17] Thomas Kämpke, Boris Kluge, Erwin Prassler, and Matthias Strobel. Robot position estimation on a RFID-tagged smart floor. In Christian Laugier and Roland Siegwart, editors, *Field and Service Robotics*, volume 42 of *Springer Tracts in Advanced Robotics*, pages 201–211. Springer Berlin Heidelberg, 2008.
- [18] K. Kodaka and S. Sugano. Reader antennas’ configuration effects for two wheeled robots on floor-installed RFID infrastructure – analysis of forward-backward configuration effect. In *Intelligent Robots and Systems (IROS), 2010 IEEE/RSJ International Conference on*, pages 5718–5724, 2010.
- [19] Dae-Sung Seo, Daeheui Won, Gwang-Woong Yang, Moo-Sung Choi, Sang-Ju Kwon, and Joon Woo Park. A probabilistic approach for mobile robot localization under RFID tag infrastructures. In *Proceedings of the 2005 International Conference on Control Automation and Systems*, pages 1797–1801, 2005.
- [20] Soonshin Han, HyungSoo Lim, and JangMyung Lee. An efficient localization scheme for a differential-driving mobile robot based on RFID system. *Industrial Electronics, IEEE Transactions on*, 54(6):3362–3369, 2007.
- [21] Sungbok Kim and Hyunbin Kim. Pseudorandom tag arrangement for accurate RFID based mobile robot localization. In Stevan Preradovic, editor, *Advanced Radio Frequency Identification Design and Applications*. InTech, 2011.
- [22] Soohee Han, Junghwan Kim, Choung-Hwan Park, Hee-Cheon Yoon, and Joon Heo. Optimal detection range of RFID tag for RFID-based positioning system using the k-nn algorithm. *Sensors*, 9(6):4543–4558, 2009.
- [23] Sunhong Park and Shuji Hashimoto. An intelligent localization algorithm using read time of RFID system. *Advanced Engineering Informatics*, 24(4):490–497, 2010.
- [24] Hyun-Jeong Lee and Hyun-Jeong Lee. Localization of mobile robot based on radio frequency identification devices. In *SICE-ICASE, 2006. International Joint Conference*, pages 5934–5939, 2006.
- [25] K. Kodaka, H. Niwa, Y. Sakamoto, M. Otake, Y. Kanemori, and S. Sugano. Pose estimation of a mobile robot on a lattice of RFID tags. In *Intelligent Robots and Systems, 2008. IROS 2008. IEEE/RSJ International Conference on*, pages 1385–1390, 2008.
- [26] Byoung-Suk Choi, Joon-Woo Lee, Ju-Jang Lee, and Kyoung-Taik Park. A hierarchical algorithm for indoor mobile robot localization using RFID sensor fusion. *Industrial Electronics, IEEE Transactions on*, 58(6):2226–2235, 2011.
- [27] D. Heß, F. Künemund, and C. Röhrig. Linux based control framework for mecanum based omnidirectional automated guided vehicles. In *Proceedings of the World Congress on Engineering and Computer Science (WCECS’13)*, pages 395–400, San Francisco, USA, October 2013.
- [28] P. F. Muir. *Modeling and Control of Wheeled Mobile Robots*. PhD thesis, Carnegie Mellon University, 1988.
- [29] Renwick E. Curry. *Estimation and Control with Quantized Measurements*. MIT Press Cambridge, 1970.